PHYSICAL REVIEW D **86,** 094502 (2012)

New ways to determine low-energy constants with Wilson fermions

P. H. Damgaard
Niels Bohr International Academy and Discovery Center, Niels Bohr Institute, University of Copenhagen, Blegdamsvej 17, DK-2100 Copenhagen Ø, Denmark

U. M. Heller
American Physical Society, One Research Road, Ridge, New York 11961, USA

K. Splittorff
Discovery Center, Niels Bohr Institute, University of Copenhagen, Blegdamsvej 17, DK-2100 Copenhagen Ø, Denmark

(Received 3 July 2012; published 5 November 2012)

We show how the leading physical and Wilson low-energy constants associated with Wilson fermions in lattice gauge theory can be determined individually by using spectral information of the Wilson Dirac operator with fixed index at finite volume. The methods are demonstrated in simulations with leading-order improved Wilson fermions. In addition to the expected suppression of the leading term in Wilson chiral perturbation theory we observe a substantial reduction also of the higher-order Wilson low-energy constants.

DOI: 10.1103/PhysRevD.86.094502 PACS numbers: 11.15.Ha, 11.30.Rd, 12.39.Fe

I. INTRODUCTION

One of the challenges facing lattice gauge theory simulations near the chiral limit is how to disentangle ultraviolet lattice artifacts from chiral behavior. As simulations with Wilson fermions approach the physical point of almost massless u and d quarks [1–5], this obstruction needs to be overcome. The traditional method is to proceed through the Symanzik effective continuum field theory, which includes a series expansion in the lattice spacing a. Associated with each power of a is a set of higher-dimensional operators whose transformation properties under chiral rotations determine the effective low-energy field theory, Wilson chiral perturbation theory. This program has been carried out to high order [6]. For a nice review, see, e.g., Ref. [7].

From the numerical point of view, the introduction of a whole new set of Wilson low-energy constants in addition to the physical low-energy parameters of QCD is, however, a challenge. One has to deal with several new fitting parameters, and hence the need to fit more observables. Moreover, for typical observables in the so-called p regime of Wilson chiral perturbation theory, one finds that observables tend to depend on particular combinations of the Wilson low-energy constants, not directly on their individual values.

In this paper, we wish to advocate a new strategy towards determining the leading physical and Wilson low-energy constants which is based on the new analytical results for spectral correlators of the Wilson-Dirac operator [8–15]. The idea is very simple, and relies on using the wealth of detailed information contained in the spectral density and spectral correlation functions of the Wilson Dirac operator D_W and its Hermitian counterpart D_5. Here, as in earlier work on how to determine QCD low-energy constants based on the Dirac operator spectrum [16], the fact that one has a new finite-volume scaling regime plays a crucial role in increasing the accuracy of the method. In particular, we shall demonstrate how the chiral condensate, the quark mass and the Wilson low-energy constants W_6, W_7 and W_8 can be obtained from the Wilson Dirac spectrum. It is central for this method that one can divide lattice configurations into sectors of fixed index ν, as determined by the spectral flow [17]. When combined with more traditional approaches from determining combinations of Wilson low-energy constants in the p regime by measuring, e.g., small differences in the charged and neutral pion masses [18,19] or from other combinations of correlation functions [20], one has a series of strong consistency checks on the obtained values.

Perturbative results for the effect of $O(a^2)$ terms on the spectrum have been compared to numerical simulations and used to determine Wilson low-energy constants in Ref. [21]. There have also been two initial studies of the detailed analytical predictions for the Wilson Dirac operator spectrum [22,23], results of which already looked promising. Here we explore the effect of introducing a simple $\mathcal{O}(a)$ clover improvement [24], using the coefficient given by leading-order weak-coupling perturbation theory. As we shall demonstrate below, one of the unexpected consequences of this simple $\mathcal{O}(a)$ improvement is that also $\mathcal{O}(a^2)$ low-energy constants of Wilson chiral perturbation theory are substantially reduced. Moreover, certain asymmetries in the data of Refs. [22,23] that clearly could not be explained by Wilson chiral perturbation theory up to, and including, $\mathcal{O}(a^2)$ effects are also substantially reduced by this clover improvement. This shows that

simple clover improvement even reduces the terms of order $\mathcal{O}(am)$, where m is the quark mass. This is good news for lattice simulations, and a result that could not have been anticipated *a priori*. All numerical data in this paper refer to the quenched approximation. It would obviously be of interest to have a confirmation of our results with the fermion determinant included.

Our paper is organized as follows. In the next section, we briefly review the theoretical setting and introduce our lattice setup. In Sec. III, we present our new numerical results, and explain how different observables can be used to probe individual Wilson low-energy coefficients. We end in Sec. IV with conclusions and an outlook for future work.

II. THE THEORETICAL FRAMEWORK

The essential input that allows us to compute the effects of $\mathcal{O}(a^2)$ on the Wilson Dirac operator spectrum is the consistency, shown by Sharpe [25], of the method up to contact terms of order am. As in Refs. [8,9], we use the ϵ-regime counting where $m \sim \epsilon^4$ and $a \sim \epsilon^2$, keeping terms up to and including $\mathcal{O}(\epsilon^4)$ (the different possible counting rules have been discussed in Ref. [26]). In the language of finite-size scaling, it means that we are considering a regime in which

$$mV, \qquad zV, \qquad a^2V,$$

are kept fixed. Here z is a source of the pseudoscalar density $\bar{\psi}\gamma_5\psi$.

Using the convention of Refs. [8,9], we write the effective Lagrangian up to that order as

$$\begin{aligned}\mathcal{L}(U) = &\frac{1}{2}(m+z)\Sigma \mathrm{Tr}U + \frac{1}{2}(m-z)\Sigma \mathrm{Tr}U^\dagger \\ &- a^2 W_6[\mathrm{Tr}(U+U^\dagger)]^2 - a^2 W_7[\mathrm{Tr}(U-U^\dagger)]^2 \\ &- a^2 W_8 \mathrm{Tr}(U^2 + U^{\dagger 2}),\end{aligned} \tag{1}$$

and we define the partition function in sectors of fixed index ν by

$$Z^\nu_{N_f}(m,z;a) = \int_{U(N_f)} dU \det{}^\nu U e^{-V\mathcal{L}(U)}. \tag{2}$$

The quenched or partially quenched limits are defined in the usual way. Operationally, the separation into sectors of fixed index ν as given above corresponds to a separation based on the spectral flow of the Wilson Dirac operator [9]. This gives a double motivation for following the spectral flow numerically, since it also provides us with the real eigenvalues of the Wilson Dirac operator D_W (see below).

We denote the usual Hermitian Wilson Dirac operator by D_5:

$$D_5 \equiv \gamma_5(D_W + m). \tag{3}$$

The source z introduced above couples to $\bar{\psi}\gamma^5\psi$. It is useful because the fermion determinant of the QCD path integral is then, up to a sign, given by

$$\det(\gamma_5(D_W+m)+z) = \det(D_5+z). \tag{4}$$

This prompts one to consider the spectral resolvent of the Hermitian Wilson Dirac operator D_5,

$$G(z) \equiv \left\langle \mathrm{Tr}\left(\frac{1}{D_5 + z - i\epsilon}\right)\right\rangle = \left\langle \sum_k \frac{1}{\lambda_k^5 + z - i\epsilon}\right\rangle, \tag{5}$$

where λ_k^5 are the eigenvalues of D_5. From this, the density of eigenvalues of D_5 follows:

$$\rho_5(\lambda^5) = \frac{1}{\pi}\,\mathrm{Im}[G(-\lambda^5)]|_{\epsilon\to 0+}. \tag{6}$$

Let us now briefly review some basic facts about the eigenvalues of D_W and D_5 [9], many of which follow directly from the early paper [27]. As is well known, eigenvalues of D_W are either real or come in complex conjugate pairs. The real eigenvalues of D_W play particularly important roles, since they provide a definition of gauge field topology as the lattice spacing a is taken to zero. Even at nonzero lattice spacing these real modes are special. It follows from the definition of D_5 that its eigenvalues λ^5 are functions of the mass m: $\lambda^5 = \lambda^5(m)$. Tuning m to a value m_c at which a zero eigenvalue occurs, $\lambda^5(m_c) = 0$, is particularly interesting since

$$D_5\phi = 0 \Rightarrow D_W\phi = -m_c\phi. \tag{7}$$

This shows that finding a zero of $\lambda^5(m)$ corresponds to identifying a real mode of D_W. It is straightforward to see that the argument runs both ways, so that a real eigenvalue of D_W also corresponds to a zero of $\lambda^5(m)$. Moreover, in a compact notation, one can show that for given eigenstates $|j\rangle$ of real modes of D_W [9,27],

$$\left.\frac{d\lambda_j^5(m)}{dm}\right|_{m=m_c} = \langle j|\gamma_5|j\rangle, \tag{8}$$

so that the slope at a crossing of the spectral flow is given by the chirality of the state $|j\rangle$. As the continuum is approached, this chirality goes to ± 1. At any finite lattice spacing the chirality vanishes identically for all nonreal modes [27].

The chirality of the real modes is also directly related to the index ν described above since around the physical branch [9],

$$\sum_{\mathrm{real}} \mathrm{sign}\langle j|\gamma_5|j\rangle = \nu, \tag{9}$$

a relation which displays the topological nature of the index: the number of zero crossings, counted with signs. As the lattice spacing a is reduced the number of multiple crossings near the physical branch of the spectrum goes to zero. On typical configurations in the present study, the definition of ν given by the spectral flow as shown above

agreed with the (improved) naive topological charge of the so-called "Boulder method," [28] which we applied after six hypercubic (HYP) smearings to the gauge fields. The few cases were the two determinations differed were usually associated with multiple crossings, with the last one at a fairly large $\lambda^W_{\rm real}$.

We now remind the reader of a few basic facts about the spectrum of the Hermitian Wilson Dirac operator [17]. In the continuum, the spectrum of the Dirac operator D is *chiral*: for every nonzero eigenvalue $i\lambda$ there is a matching eigenvalue $-i\lambda$. This holds configuration by configuration, and is a simple consequence of the γ-matrix identity $\{\gamma^\mu, \gamma^5\} = 0$. The corresponding Hermitian Dirac operator $\gamma^5(D + m)$ is also chirally symmetric:

$$\gamma^5(D + m)\phi_\pm = \pm\sqrt{\lambda^2 + m^2}\phi_\pm, \tag{10}$$

and the pairing is preserved: for every eigenvalue pair $\pm i\lambda$ of D there is a pair of eigenvalues $\pm\sqrt{\lambda^2 + m^2}$. For the zero modes of D, where there is no chiral pairing, there is also no pairing of eigenvalues of $\gamma^5(D + m)$: these eigenvalues become either $+m$ or $-m$, depending on their chiralities. The zero modes of D are chiral eigenstates. For the Wilson Dirac operator D_W these properties are violated. In particular, the spectrum of D_W is in the complex plane and it is not chirally paired. Likewise, the spectrum of $D_5 = \gamma^5(D_W + m)$ is not symmetric configuration by configuration, although the density $\rho_5(\lambda^5)$ is symmetric in the $\nu = 0$ sector.

Analytical predictions for the quenched spectrum of D_5 have been given in Refs. [8,9], although focus there was on the simplifying case when only W_8 is considered nonvanishing. General analytical expressions including W_6, W_7 and W_8 were also provided in those references. The constants W_6, W_7, and W_8 have fixed signs [8,9,13,20]: Only for W_6, $W_7 < 0$ and $W_8 > 0$ is Wilson chiral perturbation theory the effective theory of lattice QCD with a γ_5-Hermitian Wilson Dirac operator.

For the clover-improved case studied here, we shall find that $a\sqrt{|W_i|V} \ll 1$. In that case ρ_5 depends only on the combination $|W_6| + |W_7|$ rather than on W_6 and W_7 separately [9]. We shall therefore keep $W_7 = 0$ throughout the rest of this paper, and show how we can disentangle the dependence on W_6 from that on W_8.

III. SIMULATIONS AND NUMERICAL RESULTS

We use two of the gauge field ensembles already considered in our previous work [22]. Both were generated with the Iwasaki gauge action [29] and have a lattice size of $L = 1.5$ fm. Some further properties are given in Table I, including the lattice spacing inferred from r_0/a values from [30,31] using $r_0 = 0.5$ fm to set the physical scale, and the number of configurations analyzed with $|\nu| = 0$, 1, and 2. We have applied one HYP smearing [32] to the gauge fields before constructing the clover Dirac operator

TABLE I. Ensemble of pure gauge configurations considered, generated with the Iwasaki gauge action. Listed are β_{Iw}, the size in lattice units, the lattice spacing, the bare mass in the clover Dirac operator and the number of configurations in the sectors with $|\nu| = 0$, 1, and 2.

β_{Iw}	Size	a [fm]	am_0	$\nu = 0$	$\lvert\nu\rvert = 1$	$\lvert\nu\rvert = 2$
2.635	16^4	0.093	−0.03	1276	2257	1518
2.79	20^4	0.075	−0.027	1202	2128	1408

with the tree-level clover coefficient $c_{sw} = 1$. It is known [33] that the tree-level clover coefficient is fairly close to a nonperturbatively improved value when using HYP smeared gauge fields.

We now turn to an analysis of our lattice data. We start by numerical results obtained on the 16^4 lattice. As a first test of the impact of clover improvement, we show in Fig. 1 the density of real modes of D_W in the $\nu = 1$ sector. On the same plot is shown earlier data from Ref. [22] *without* clover improvement. It is evident that clover improvement as expected shifts the position of the peak towards the origin. Moreover, it is also clear that the clover improvement has reduced the width of the peak substantially. In the analytic computation within Wilson chiral perturbation theory [8,9] this width is determined by the terms of order a^2. Hence we conclude that the clover term also has a positive effect on the order a^2 terms. Finally, the fact that the peak has become more symmetric must necessarily be due to an improvement of the terms of order $\mathcal{O}(am) \sim \epsilon^6$ and higher. As our analytical results extend only to order ϵ^4 we unfortunately cannot quantify this suppression of the asymmetry further. Overall this seems to show that clover improvement works better than we had reasons to expect, see also Ref. [34]. We now turn to the effect of clover improvement on the spectrum of D_5. Since in the small-a

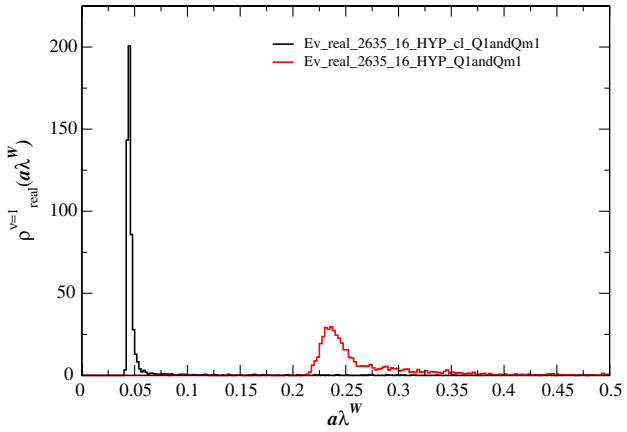

FIG. 1 (color online). The effect of clover improvement on the density of the real eigenvalues of D_W. The black line is the clover improved data and the red (gray) line is the data before clover improvement. Not only does the peak shift towards the origin, the clover term also makes it much more narrow and symmetric.

limit the real eigenvalues of D_W map directly to the peak at $\lambda^5 = m$, we certainly expect improvement here as well.

The histograms in Fig. 2 give the eigenvalue density of the Hermitian Wilson Dirac operator in the $\nu = 0$, 1 and 2 sectors as obtained from the 16^4 lattices. Displayed also are two fits of the analytic curves obtained from Wilson chiral perturbation theory. With the additional Wilson low-energy constants there are in total 5 parameters to fit ($\Sigma V/a$, $m\Sigma V$, $W_6 a^2 V$, $W_7 a^2 V$ and $W_8 a^2 V$). Fortunately the analytic results of Refs. [9,22] give us a series of insights that allow us to address these constants in turn. First of all, as mentioned above, the Wilson low-energy constants W_i have fixed signs $W_6 < 0$, $W_7 < 0$ and $W_8 > 0$ [8,9,13,20]. Moreover, [9,10] in the limit where $a\sqrt{|W_i|V} \ll 1$ there is a factorization of the eigenmodes of D_5, while those in the index peak have a specific dependence on the W_i's the rest of the eigenvalue density is not affected to leading order in $a\sqrt{|W_i|V}$, see Fig. 6 below for an illustration. This has the following most useful consequences:

(1) The eigenvalue density on the opposite side of the index peak is almost continuumlike.
(2) The smallest eigenvalues on this side of the origin are located very close to $-m$ and thus offer a clean way to extract the quark mass parameter.
(3) The value of Σ can be estimated by scaling the λ^5 axis and m until the data on this side of the gap match the continuum predictions.
(4) The values of the W_i's are finally obtained from their effect on the index peak (see below).

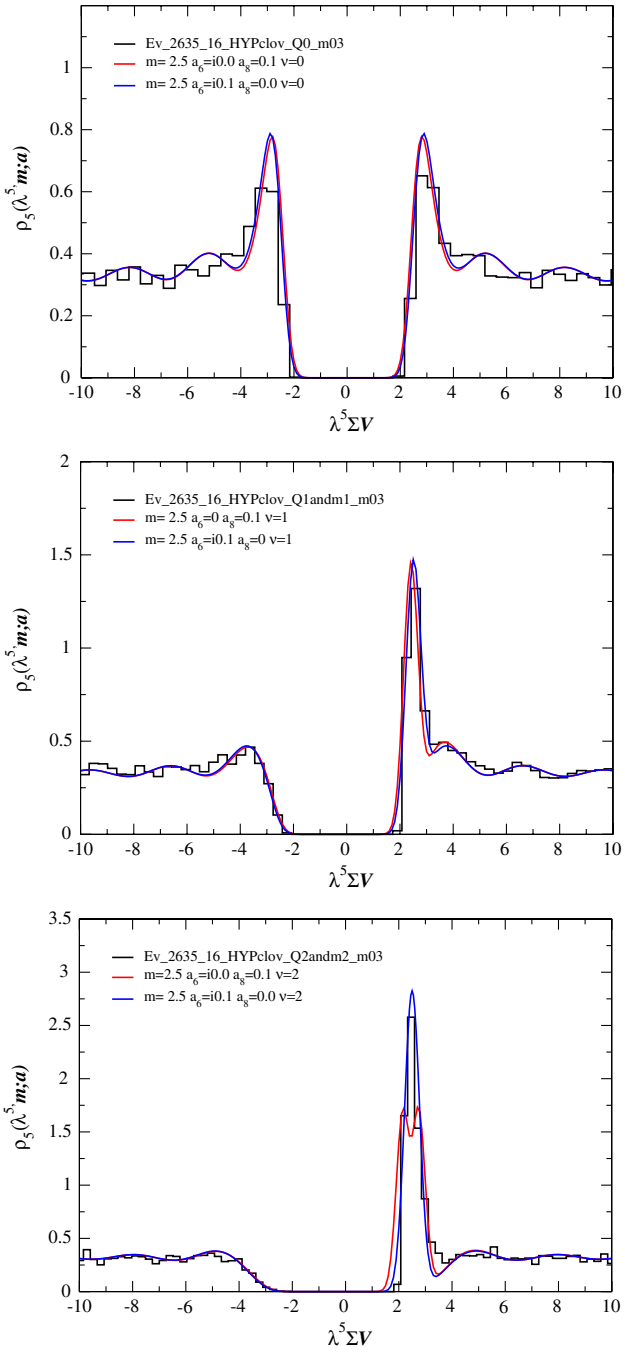

FIG. 2 (color online). The spectral density of the Hermitian Wilson Dirac operator on the 16^4 lattices. The numerically determined eigenvalues have been rescaled with $\Sigma V/a = 173$ for the comparison to the analytic results. The $|\nu| = 2$ data in the lower panel allow us to separate the effect of W_6 from that of W_8.

The fits were made, using the above insights, to the $|\nu| = 1$ data and have $a\sqrt{-W_6 V} = 0.1$ and $W_8 = 0$ (blue line) respectively $W_6 = 0$ and $a\sqrt{W_8 V} = 0.1$ (red line). In both cases $\Sigma V/a = 173$ and $m\Sigma V = 2.5$.

As can be seen from the middle panel of Fig. 2 the $|\nu| = 1$ data work well both with W_6 alone (blue curve) and with W_8 alone (red curve).

Having fixed the values of the low-energy constants by the $|\nu| = 1$ data we can now check the two corresponding predictions from Wilson chiral perturbation theory against the $\nu = 0$ and $|\nu| = 2$ data. In the top panel for $\nu = 0$ both predictions do well, however, for the $|\nu| = 2$ data only the prediction from the fit with W_6 alone reproduces the peak structure of the would-be topological modes.

In Fig. 3, we plot the analytic predictions (the values of the low-energy constants still fixed as above) for the real eigenvalues of the Wilson Dirac operator against the real eigenvalues of the $|\nu| = 1$ and $|\nu| = 2$ sectors. In the top panel the red lines display the predictions corresponding to the fit with W_8 alone. The predictions from the fit with W_6 alone are given in the lower panel (blue lines). Again the $|\nu| = 2$ data for the real eigenvalues clearly favors the prediction with W_6 alone.

The reason why W_6 and W_8 have such a different effect on the analytic prediction with $|\nu| = 2$ is the following: The W_6-term in the ϵ regime of Wilson chiral perturbation theory corresponds to a Gaussian fluctuating mass [9]. The δ peak from the continuum at m is therefore smeared into a Gaussian with an amplitude that simply scales with ν. In particular, W_6 does not induce eigenvalue repulsion between the real modes. On the contrary it was shown in

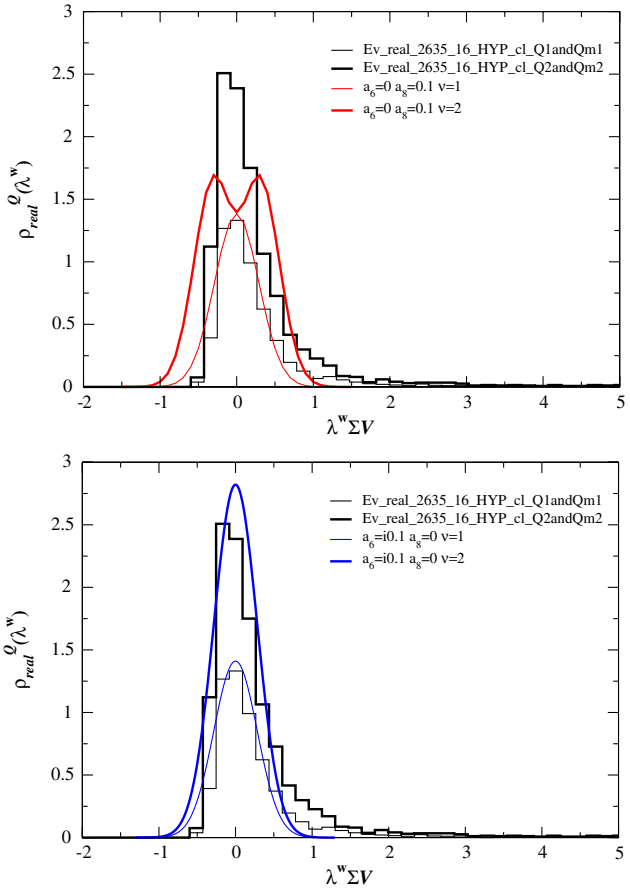

FIG. 3 (color online). The density of the real eigenvalues of D_W, rescaled with $\Sigma V/a = 173$. Clearly the prediction with $W_8 = 0$ (blue lines lower panel) gives the better description of the $|\nu| = 2$ data.

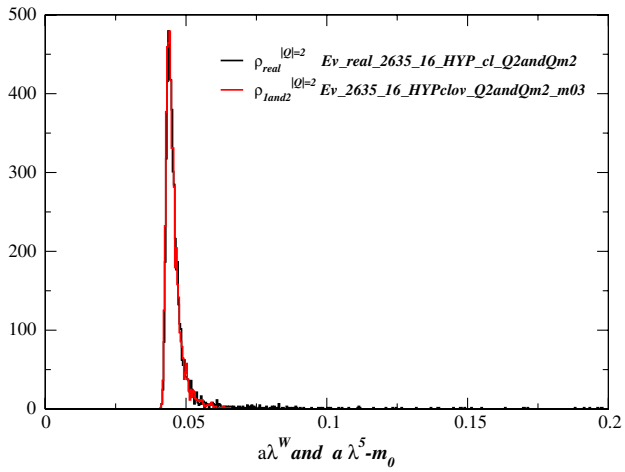

FIG. 4 (color online). The density of the real eigenvalues of D_W for $|\nu| = 2$ on the 16^4 lattice plotted together with the accumulated density of the first two positive eigenvalues of D_5 on the same configurations shifted by the bare mass. The excellent match between the two demonstrates that the corresponding eigenvectors are almost chiral.

Refs. [9,10] that for small but nonzero a^2W_8V the density of the real eigenvalues of D_W takes the form of the $\nu \times \nu$ Gaussian unitary ensemble scaled by $4a^2W_8V$. The effect of W_8 is therefore to induce the eigenvalue repulsion familiar from random matrix theory between the real

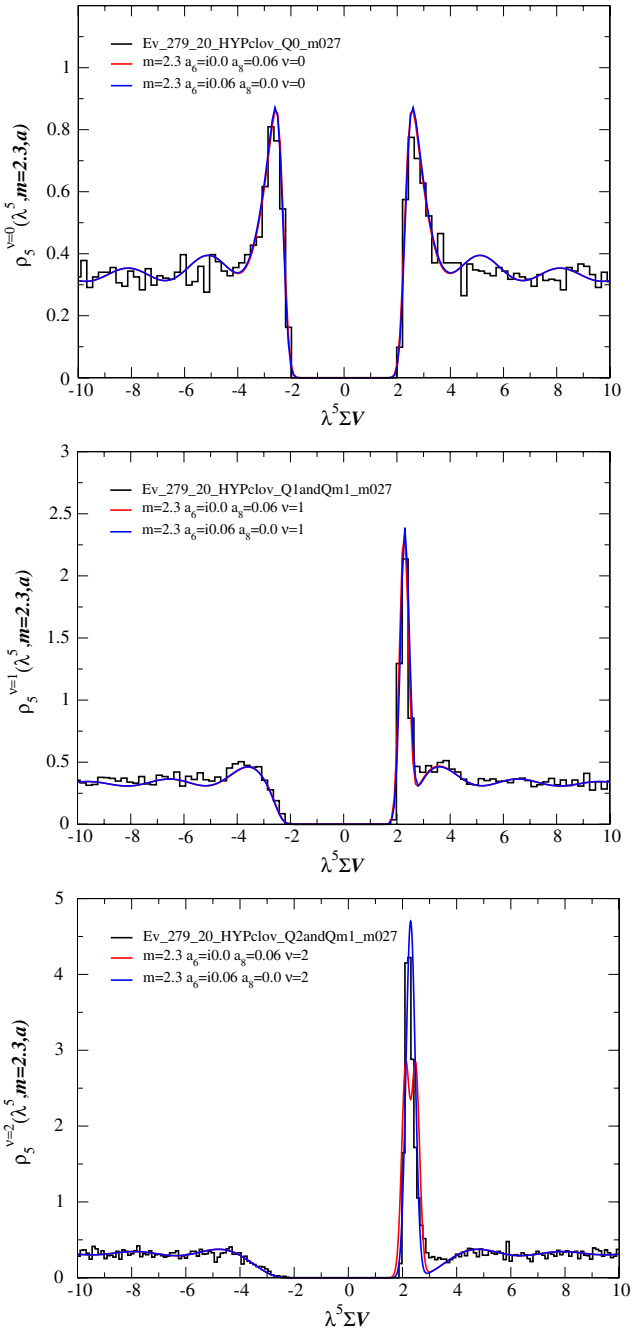

FIG. 5 (color online). The spectral density of the Hermitian Wilson Dirac operator on the 20^4 lattices. The eigenvalues have been rescaled with $\Sigma V/a = 220$. In blue and red are two fits (see the main text) to the $|\nu| = 1$ data in the middle panel. In the top and lower panel the predictions obtained from these fits are plotted against the data.

modes. In this way, we get a clear distinction between the effect of W_6 and W_8.

The fact that the real modes of D_W and the nearly topological peak in the spectrum of D_5 both lead to the same conclusion is not accidental. In Fig. 4, we plot the real modes of D_W for $|\nu| = 2$ together with the distribution of the first two positive eigenvalues of D_5 appropriately shifted by the bare mass. The essentially perfect match between the two distributions demonstrates that the corresponding eigenvectors are almost chiral as is expected for $|a^2 W_i V| \ll 1$, see Fig. 4 of Ref. [9] and the associated discussion.

Let us now consider the 20^4 data set. In Fig. 5, the eigenvalue density of the Hermitian Wilson Dirac operator is displayed for $\nu = 0$ (top panel), $|\nu| = 1$ (middle panel) and $|\nu| = 2$ (lower panel). Again we have made two fits to the $|\nu| = 1$ data, one with $W_8 = 0$ (blue line) and one with $W_6 = 0$ (red line). The values in this case are $a\sqrt{-W_6 V} = 0.06$ and $W_8 = 0$ (blue line), respectively, $W_6 = 0$ and $a\sqrt{W_8 V} = 0.06$ (red line) both with $\Sigma V/a = 220$ and $m\Sigma V = 2.3$.

These values were determined according to the strategy outlined above. To illustrate the factorization of the behavior used we show in Fig. 6 the fit for $\nu = 1$ and $W_8 = 0$ together with the continuum, $a = 0$, curve at the same quark mass. As is clear, the leading-order effect for $a\sqrt{|W_i|V} \ll 1$ is on the index peak only.

The two fits both describe the $|\nu| = 1$ data well and the prediction for $|\nu| = 0$ also works nicely for both fits. For $|\nu| = 2$ the analytic predictions again differ in the region of the topological modes. Also here it is the prediction with W_6 alone that gives the only acceptable fit to the $|\nu| = 2$ data. This again allows us to conclude that W_6 gives the dominant contribution to the discrepancy from the continuum.

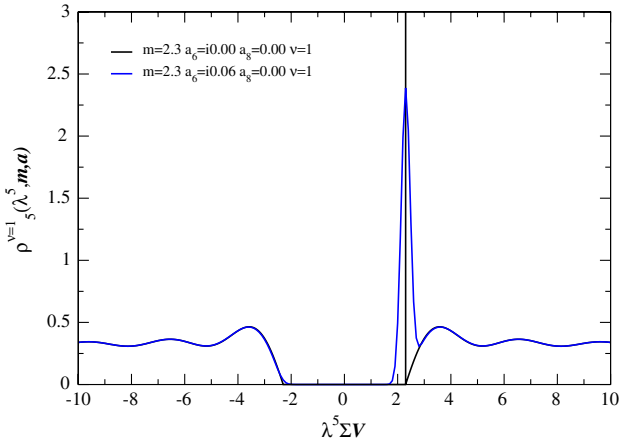

FIG. 6 (color online). Comparison of the microscopic eigenvalue density of the Hermitian Wilson Dirac operator in the continuum $a = 0$ (black curve) and with $a\sqrt{W_6 V} = i0.06$, $W_8 = 0$ (blue curve). The vertical black line indicates the position of the topological δ peak. To leading order in $a\sqrt{|W_i|V}$ only this peak is affected by the discretization.

Finally, to summarize the effect of clover improvement: Before clover improvement [22] we found that the values of $a\sqrt{|W_8|V}$ were roughly 0.35 for both the 16^4 and 20^4 lattices. Here, after clover improvement, we find that $a\sqrt{|W_8|V}$ is consistent with zero and that $a\sqrt{|W_6|V}$ takes the values 0.10 and 0.06, respectively. Moreover, the asymmetry of the density of the real modes has been substantially reduced by the addition of the clover term. This indicates an improvement also at order $\mathcal{O}(am)$. While this unexpected order $\mathcal{O}(a^2)$ and $\mathcal{O}(am)$ improvement is an analytic challenge to understand, it is clearly good news for lattice QCD.

IV. CONCLUSIONS AND OUTLOOK

We have shown how the microscopic eigenvalue density of the Wilson Dirac operator can be used to determine both physical and lattice-artifact low-energy constants from lattice QCD simulations. We have demonstrated this with quenched clover-improved simulations. The method relies crucially on our ability to divide the lattice configurations into sectors with fixed index.

While initial numerical tests [22,23] had already demonstrated the feasibility of computing the microscopic spectrum of the Wilson Dirac operator and comparing it to analytical predictions, there were aspects of the measured spectra that displayed a systematic disagreement with the analytical predictions. In particular, the observed asymmetry in the spectrum of the real modes of D_W. This asymmetry has been known to be present in data from very early on, and yet it is a firm prediction of Wilson chiral perturbation theory up to and including $\mathcal{O}(a^2)$ that the spectrum must be symmetric. A quick analysis reveals that terms involving odd powers of am in the effective theory are needed to explain such an asymmetry. This is beyond present analytical predictions. Here we have improved at order a through use of the conventional clover term. Since the effective theory contains an arbitrary linear shift in the mass term anyway, such an improvement is, in this context, not interesting in itself. But clearly clover improvement has an impact on higher-order coefficients as well. We have found that clover improvement in fact substantially reduces the higher-order Wilson constants *and* makes the spectrum of real modes much more symmetric, and hence in good agreement with analytical predictions. Because of the close connection between real modes of D_W and the "topological" (threshold) eigenvalues of D_5, this improves the eigenvalue spectrum of D_5 as well.

Apart from demonstrating substantially better agreement between theory and numerical data, we have taken the opportunity to explain new ways to measure Wilson low-energy constants based on spectral data of the Wilson Dirac operator. In particular, we have shown how a detailed

understanding of how the different $\mathcal{O}(a^2)$ operators in the Wilson chiral Lagrangian influence the spectrum can be used to isolate dependencies on the individual low-energy constants. This should be very helpful in determining the numerical values of the constants in dynamical simulations. Crucial in this context is the separation of configurations into sectors of fixed index ν, the Wilson analogue of a topological charge. In each sector there are definite predictions with which to compare the data.

The present study should be extended to full-scale simulations with dynamical fermions. Analytical predictions are already available for two light flavors [12]. This gives entirely new ways to measure the low-energy constants of Wilson chiral perturbation theory that can be compared to and combined with alternative approaches using more conventional space-time dependent observables in the p regime. Although computationally more complicated, it would also be most interesting to carry out analogous studies of the full complex spectrum of D_W. The analytical predictions are available in Refs. [11,13]. In particular, the realization of either the Aoki phase [35] or the Sharpe-Singleton scenario [6] is closely linked to the complex spectrum of D_W [13].

Finally, due to the unexpected higher order improvement caused by the clover term it would be interesting to test the effect of clover improvement also in twisted mass lattice QCD. As we have demonstrated here, the spectral density of the lattice Dirac operator is an efficient tool for such an analysis. The necessary analytical predictions from Wilson chiral perturbation with a maximally twisted mass have recently been derived [36].

ACKNOWLEDGMENTS

We thank Jac Verbaarschot, Urs Wenger, and Silvia Necco for discussions. P. H. D. and K. S. would like to thank the CERN theory group for discussions and hospitality while this work was completed. The work of K. S. was supported by the *Sapere Aude* program of The Danish Council for Independent Research.

[1] L. Del Debbio, L. Giusti, M. Lüscher, R. Petronzio, and N. Tantalo, J. High Energy Phys. 02 (2007) 056; J. High Energy Phys. 02 (2007) 082.
[2] R. Baron *et al.* (ETM Collaboration), Proc. Sci. LATTICE2008 (2008) 094.
[3] T. Ishikawa *et al.* (JLQCD Collaboration), Phys. Rev. D **78**, 011502 (2008).
[4] S. Aoki *et al.* (PACS-CS Collaboration), Phys. Rev. D **81**, 074503 (2010).
[5] S. Durr, Z. Fodor, C. Hoelbling, S. D. Katz, S. Krieg, T. Kurth, L. Lellouch, T. Lippert, K. K. Szabó, and G. Vulvert, J. High Energy Phys. 08 (2011) 148; Phys. Lett. B **701**, 265 (2011).
[6] S. Sharpe and R. L. Singleton, Phys. Rev. D **58**, 074501 (1998); G. Rupak and N. Shoresh, Phys. Rev. D **66**, 054503 (2002); O. Bär, G. Rupak, and N. Shoresh, Phys. Rev. D **70**, 034508 (2004); S. Aoki, Phys. Rev. D **68**, 054508 (2003); S. Aoki and O. Bär, Phys. Rev. D **70**, 116011 (2004).
[7] M. Golterman, arXiv:0912.4042.
[8] P. H. Damgaard, K. Splittorff, and J. J. M. Verbaarschot, Phys. Rev. Lett. **105**, 162002 (2010).
[9] G. Akemann, P. H. Damgaard, K. Splittorff, and J. J. M. Verbaarschot, Phys. Rev. D **83**, 085014 (2011).
[10] G. Akemann and T. Nagao, J. High Energy Phys. 10 (2011) 060.
[11] M. Kieburg, J. J. M. Verbaarschot, and S. Zafeiropoulos, Phys. Rev. Lett. **108**, 022001 (2012).
[12] K. Splittorff and J. J. M. Verbaarschot, Phys. Rev. D **84**, 065031 (2011).
[13] M. Kieburg, K. Splittorf,f and J. J. M. Verbaarschot, Phys. Rev. D **85**, 094011 (2012).
[14] G. Akemann and A. C. Ipsen, J. High Energy Phys. 04 (2012) 102.
[15] M. Kieburg, J. Phys. A **45**, 205203 (2012).
[16] G. Akemann and A. C. Ipsen, J. Phys. A **45**, 115205 (2012); C. Lehner, S. Hashimoto, and T. Wettig, J. High Energy Phys. 06 (2010) 028; P. H. Damgaard, U. M. Heller, K. Splittorff, B. Svetitsky, and D. Toublan, Phys. Rev. D **73**, 074023 (2006); Phys. Rev. D **73**, 105016 (2006); P. H. Damgaard, U. M. Heller, K. Splittorff, and B. Svetitsky, Phys. Rev. D **72**, 091501 (2005).
[17] R. G. Edwards, U. M. Heller, and R. Narayanan, Nucl. Phys. **B535**, 403 (1998); Phys. Rev. D **60**, 034502 (1999); K. M. Bitar, U. M. Heller, and R. Narayanan, Phys. Lett. B **418**, 167 (1998).
[18] L. Scorzato, Eur. Phys. J. C **37**, 445 (2004).
[19] R. Baron *et al.* (ETM Collaboration), J. High Energy Phys. 08 (2010) 097.
[20] M. T. Hansen and S. Sharpe, Phys. Rev. D **85**, 014503 (2012); Phys. Rev. D **85**, 054504 (2012).
[21] S. Necco and A. Shindler, J. High Energy Phys. 04 (2011) 031; Proc. Sci. LATTICE 2011 (2011) 250.
[22] P. H. Damgaard, U. M. Heller, and K. Splittorff, Phys. Rev. D **85**, 014505 (2012).
[23] A. Deuzeman, U. Wenger, and J. Wuilloud, J. High Energy Phys. 12 (2011) 109.
[24] B. Sheikholeslami and R. Wohlert, Nucl. Phys. **B259**, 572 (1985).
[25] S. R. Sharpe, Phys. Rev. D **74**, 014512 (2006).
[26] A. Shindler, Phys. Lett. B **672**, 82 (2009); O. Bär, S. Necco, and S. Schaefer, J. High Energy Phys. 03 (2009) 006; O. Bär, S. Necco, and A. Shindler, J. High Energy Phys. 04 (2010) 053; S. Necco and A. Shindler, J. High Energy Phys. 04 (2011) 031.
[27] S. Itoh, Y. Iwasaki, and T. Yoshie, Phys. Rev. D **36**, 527 (1987).

[28] T. A. DeGrand, A. Hasenfratz, and T. G. Kovacs, Nucl. Phys. **B505**, 417 (1997).
[29] Y. Iwasaki, Report No. UTHEP-118, 1983.
[30] S. Takeda *et al.*, Phys. Rev. D **70**, 074510 (2004).
[31] S. Necco, Nucl. Phys. **B683**, 137 (2004).
[32] A. Hasenfratz and F. Knechtli, Phys. Rev. D **64**, 034504 (2001).
[33] Y. Shamir, B. Svetitsky, and E. Yurkovsky, Phys. Rev. D **83**, 097502 (2011).
[34] A. Hasenfratz, R. Hoffmann, and S. Schaefer, J. High Energy Phys. 11 (2007) 071.
[35] S. Aoki, Phys. Rev. D **30**, 2653 (1984).
[36] K. Splittorff and J. J. M. Verbaarschot, Phys. Rev. D **85**, 105008 (2012).